[9]I. Aronson, Y. Hahn, P. Henry, C. J. Kleinman, and L. Spruch, Phys. Rev. 153, 73 (1967); 161, 23 (1967).
[10]H. F. Saraph and M. J. Seaton, Proc. Phys. Soc. (London) 80, 1057 (1962).
[11]T. Kinoshita, Phys. Rev. 105, 1490 (1957); 115, 366 (1959).
[12]C. L. Pekeris, Phys. Rev. 112, 1649 (1958); 115, 1216 (1959); 126, 1470 (1962).
[13]G. Breit, Rabi Symposium, 1967, Columbia University (unpublished).
[14]Y. Hahn, Phys. Rev. 169, 794 (1968).
[15]L. D. Faddeev, Zh. Eksperim. i Teor. Fiz. 39, 1459 (1960) [English transl.: Soviet Phys. – JETP 12, 1014 (1961)].
[16]S. Weinberg, Phys. Rev. 133, B232 (1964); C. Lovelace, *ibid.* 135, B1225 (1964).
[17]Y. Hahn, Phys. Rev. (to be published), where an alternate formulation of the variational bound without the explicit use of the projection operators has been given, and exactly the same approach also applies to the present case of bound-state problems.

PHYSICAL REVIEW VOLUME 187, NUMBER 1 5 NOVEMBER 1969

Molecular-Beam Maser for the Shorter-Millimeter-Wave Region: Spectral Constants of HCN and DCN†

Frank DeLucia and Walter Gordy
Department of Physics, Duke University, Durham, North Carolina 27706
(Received 2 July 1969)

A millimeter-wave molecular-beam maser has been made to operate as both an amplifier and an oscillator on the $J=1\rightarrow 0$ and the $J=2\rightarrow 1$ transitions of HCN at 88.6 and at 177.2 kMc/sec, respectively, thus doubling the previously operational frequency range of such masers. With this maser, hyperfine components of these transitions have been measured for $H^{12}C^{14}N$ and $D^{12}C^{14}N$ to nine significant figures. The spectral constants (in kc/sec) that are derived from these frequencies are, for HCN, $B_0=44\,315\,975.7\pm0.4$, $D_J=87.24\pm0.06$, $(eQq)_N=-4709.1\pm1.3$, and $C_N=10.4\pm0.3$; for $D^{12}C^{14}N$, $B_0=36\,207\,462.7\pm0.2$, $D_J=57.83\pm0.04$, $(eQq)_N=-4703.0\pm1.2$, $C_N=8.4\pm0.3$, $(eQq)_D=194.4\pm2.2$, and $C_D=-0.6\pm0.3$.

INTRODUCTION

Molecular-beam techniques provide the highest resolution and make possible the most accurate measurement of molecular spectral frequencies of any known method. Although the beam maser was first successfully operated[1] in 1954, it has, to date, been used to measure the spectral transitions of only a few molecules, notably the inversion spectrum of ammonia, NH_3, and NH_2D, and rotational transitions of the asymmetric-top molecules H_2O, HDO, D_2O, HDS, HDSe, H_2CO, and HDCO. These transitions all occur in the centimeter-wave region. There are several reasons for this. Microwave techniques become increasingly more difficult as they are extended into the millimeter and submillimeter region, and detection sensitivity decreases rapidly. Maser techniques require transitions with relatively large populations and favorable state-selection properties. Both of these are provided by the above types of molecules. Linear and symmetric-top molecules without inversion result in either poor population (molecules with small rotational constants) or transitions outside the centimeter region (molecules with large rotational constants). The state selection is also most effective for the closely spaced doublets of the NH_3 inversion spectrum and of the light asymmetric molecules.

Two molecular-beam masers have previously been made to operate in the millimeter-wave region. Marcuse[2] succeeded in obtaining maser action, both amplification and oscillation, with the $J=1\rightarrow 0$ rotational transition of HCN at 88.6 kMc/sec, but he did not make high-precision measurements of the frequencies. Likewise, Krupnov and Skvortsov[3] constructed a molecular-beam maser which operated successfully on the $1_{01}\rightarrow 0_{00}$ transition of H_2CO at 72.8 kMc/sec, but they did not, to our knowledge, measure the spectral frequencies.

We have constructed an HCN beam maser which operates as amplifier and oscillator, not only on the hyperfine transitions of the $J=1\rightarrow 0$ transition, but also on the $J=2\rightarrow 1$ hyperfine transitions which fall at 177.2 kMc/sec. Thus we have succeeded

in doubling the operable frequency range of the molecular-beam maser. Coupled with our maser is a marker system which permits measurements of the frequencies to nine significant figures. With it, we have been able to measure the rotational constants of the ground vibrational state of HCN and DCN to a precison not previously achieved for any molecule.

In a recent development,[4] to be described in a later publication, we have extended the operation of the molecular-beam maser into the submillimeter-wave region, using the $1_{10} \rightarrow 1_{01}$ transition of D_2O at 316 kMc/sec ($\lambda = 0.95$ mm).

Gaseous lasers have been made to operate at some frequencies in the far infrared and in the submillimeter-wave regions, and frequencies of a few of them have been measured[5] with microwave techniques to a precision of 1 Mc/sec. This accuracy is not comparable to that of 1 kc/sec achieved here with the beam maser. The greater accuracy reported here is due primarily to the elimination of Doppler and pressure broadening in the molecular-beam maser.

EXPERIMENTAL ASPECTS

The apparatus used in these experiments is shown in Fig. 1. It is similar in certain respects to the conventional centimeter-wave molecular-beam maser; however, it differs in several important aspects. The most significant change is the replacement of the low-order-mode cylindrical cavity commonly used in centimeter-wave masers by a high-order-mode Fabry-Perot cavity. To take advantage of the increased frontal area presented to the beam by the Fabry-Perot cavity, the usual single molecular beam was replaced with a multiple-beam arrangement, as was done in the previous millimeter-wave masers.[2,3] These beams were formed by a number of sections of needle tubing embedded in one side of a flat, rectangular box. The state selector consists of a number of stacked quadrupole fields separated by cooled copper fins which served to trap deflected and scattered molecules and helped to maintain the vacuum necessary for the molecular beam. The cavity consists of one fixed flat plate that had a diameter of 4 in., with waveguide coupling, and one spherically curved plate mounted on a slide arrangement. The cavity was tuned by the driving of this slide with a screw arrangement connected to a rotary vacuum feedthrough. The cavity spacing is approximately semiconfocal. After the beam traversed the state selector and cavity, it was trapped on a surface cooled to the temperature of liquid nitrogen. The entire apparatus is enclosed in a vacuum chamber capable of being evacuated to about 2×10^{-6} mm Hg. This vacuum is provided by a 4-in. diffusion pump and liquid-nitrogen cold traps. These traps provide a simple and effective means for the handling of the pumping load caused by the relatively large amounts of gas in the beam.

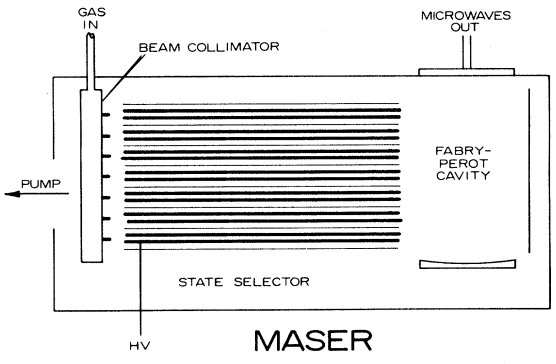

FIG. 1. Diagram of the molecular-beam maser.

The microwave measurement and detection system is shown in Fig. 2. The fundamental frequency reference was provided by a General Radio 1115-B high-stability 5-Mc/sec crystal oscillator, the frequency of which was continually compared against WWVB by a Hewlett-Packard 117A VLF receiver and phase comparator. This system is accurate to about one part in 10^{10}. The 5-Mc/sec signal from the oscillator was multiplied in an harmonic multiplier chain to 1080 Mc/sec and then mixed, along with a phase-related 180-Mc/sec signal, in a 1N26 crystal with part of the klystron output. The resulting rf signal was split into two parts. One part was fed back into an automatic frequency control loop to provide the stability in klystron frequency necessitated by the narrow maser lines. The remainder was used to provide the necessary frequency markers for measurement of the spectral line frequencies. Beating the marker signal with the output of a stable variable-frequency oscillator (VFO), rather than with the internal beat-frequency oscillator of the receiver, eliminated the error due to frequency drift of the high frequency oscillator in the marker receiver. The frequency of the VFO was measured with a counter.

The detection system is a superheterodyne receiver which employs the same klystron for harmonic mixing and harmonic generation. This system has good sensitivity and stability. Furthermore, it is simpler to use and is more economical than a system which employs separate klystrons for the two operations. The output of the klystron was split into two parts. One part was applied to a crossed-waveguide harmonic generator along with a 30-Mc/sec rf signal. The resulting sideband at $n\nu + 30$ Mc/sec ($n = 2$ or 3 for the transitions reported here) was used to stimulate the maser cavity. All other sidebands and harmonics were efficiently filtered out by the high-Q cavity. The output of the maser was mixed in a crystal harmonic mixer with the kly-

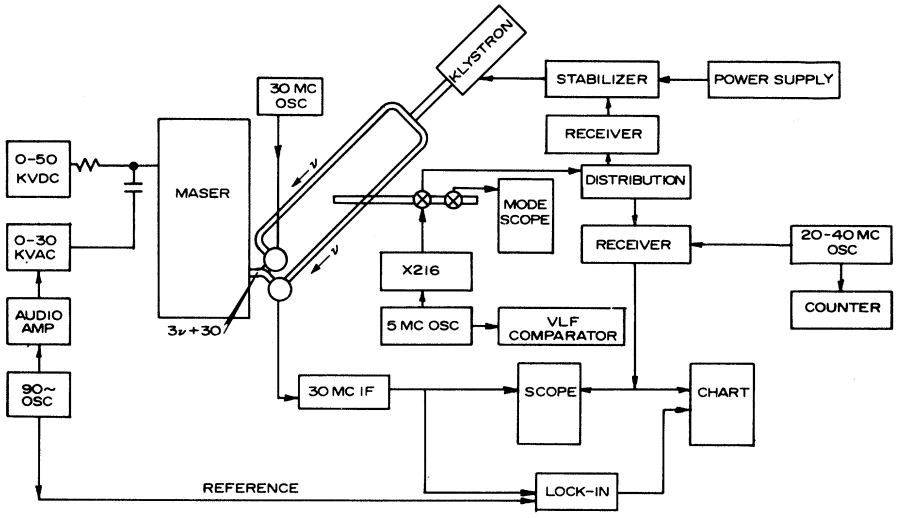

FIG. 2. Diagram of the millimeter-wave system for detection and measurement of maser output.

stron signal, and the resulting 30-Mc/sec signal was then amplified in an i.f. strip and applied either to an oscilloscope or a lock-in amplifier. With the lock-in system the reference modulation was obtained by application of a high-voltage ac signal of about 90 cps, in addition to the dc bias on the state selector. This procedure modulated the state selection, resulting in amplitude modulation of the output of the maser.

The theory of molecular-beam masers operating at centimeter wavelengths, as well as the results obtained with them, has been the subject of extensive treatment. Much of this applies also to masers operating at higher frequencies. There are, however, several significant differences which we shall discuss here. One of the most important of these is the replacement of the cylindrical cavity with a Fabry-Perot cavity. Attempts at scaling down centimeter cavities to millimeter wavelengths have not been too successful. Unfortunately for this approach, the Q is proportional to $\nu^{-1/2}$, the linewidth to ν, and the amount of beam admitted to the cavity to ν^{-2}. All of these factors have negative effects on the operation of a maser and contribute to the need for changing to another type of cavity. The Fabry-Perot cavity has high Q (in our maser, 300 000 at 88.6 kMc/sec and 500 000 at 177.2 kMc/sec), a large frontal area to admit the beam, and a sufficient spread of the microwave field to give sharp spectral lines. The large volume of the Fabry-Perot cavity cancels some of this advantage by reducing the filling factor, thus making oscillation more difficult. This disadvantage can be partially overcome by use of a multiple-beam arrangement, but usable state-selector geometries continue to result in a filling factor somewhat smaller than that of the usual centimeter-wave cavity. When all factors are considered, the Fabry-Perot cavity, at short millimeter wavelengths, is comparable in overall performance to the cylindrical cavity at centimeter wavelengths, and is much superior to the cylindrical cavity scaled down to the shorter millimeter wavelengths.

The state-selection process for low J states of linear molecules differs from that for the close-lying doublets previously used for centimeter-wave masers. Molecular-beam masers employ selective deflection of molecules in different energy states to achieve population inversion. The electric fields in quadrupole state selectors are such that molecules in states that increase in energy in a Stark field are focused into the beam, whereas those molecules in energy states that decrease are deflected out of the beam. Figure 3 shows the Stark effect on the $J=0$, 1, and 2 levels of HCN and their relative deflection in the strong-field case. Since the state selection takes place at high electric fields, the appropriate quantum numbers are m_I and m_J. However, the maser operates in zero field, where F and m_F are the appropriate quantum numbers. Thus, if the state-selection process is to be understood, the strong-field levels must be associated with the zero-field levels which they collapse into, as the electric field goes from its maximum in the state selector to zero in the cavity. In principle, one might do this by solving the intermediate-field Stark effect for several values of Stark field and following each level from high-field to low-field approximations. There is, however, an easier method. The two following rules established a unique correspondence between the two sets of quantum numbers: (a) $m_F = m_I + m_J = m$; (b) in the adiabatic transition from the zero-field states to the high-field states, states having the same m do not cross.[6]

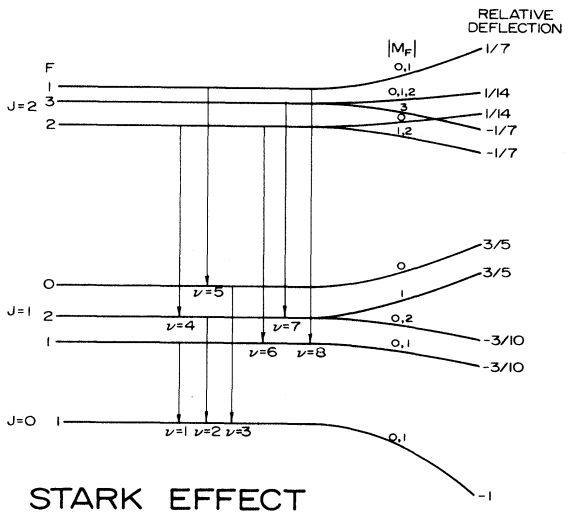

FIG. 3. Energy-level diagram showing Stark effect of HCN.

The deflection due to state selection for HCN molecules in the $J = 0$ state is approximately twice as great as that for NH_3 molecules in the $J = 3$, $K = 3$ inversion state. Thus, from Fig. 3, the transition labeled $\nu = 1$ has state selection somewhat more favorable than that of NH_3; $\nu = 2$, with part of its upper state deflected out of the beam, has about the same quality; and $\nu = 3$ has considerably worse, because both upper and lower levels are deflected out of the beam – although the lower level, fortunately, is deflected more rapidly. The state selection in $J = 2 \rightarrow 1$ is quite interesting. All of the deflections are less than those of NH_3, some considerably less. However, a new situation now occurs: Some of the $J = 2 \rightarrow 1$ hyperfine components will appear in the output as state-selected absorption lines. The transition labeled $\nu = 8$ has the ideal type of state selection for emission: The upper level is focused entirely into the beam, and the lower level, entirely out of the beam. As a result, this line is the strongest one in the maser output and was, therefore, used for the maser oscillator. It is strongest even though in absorption spectra it accounts for only 8% of the total transition intensity. Another emission line is $\nu = 6$, with its lower level deflected entirely out of the beam and its upper level exhibiting a mixed state selection. The other three components $\nu = 4$, 5, and 7 are all absorption lines. The strengths of these absorption lines are considerably enhanced by the state-selection process because the resulting population difference between their upper and lower states is considerably larger than the 3% provided by the Boltzmann distribution.

Oscilloscope tracings of the maser oscillators are shown in Fig. 4. The tracing on the left is that of the $J = 1 \rightarrow 0$ oscillator; the one on the right is that of the $J = 2 \rightarrow 1$ oscillator. They were made with a system similar to that shown in Fig. 2, except that the 30-Mc/sec signal was removed from the harmonic multiplier, and the stimulating signal was thereby removed from the maser cavity. Figure 5 shows the hyperfine tracings of the $J = 1 \rightarrow 0$ transition of DCN. Each of the pictures shows one of the nitrogen quadrupole components: The $F = 1$ and $F = 2$ levels in 5(a) and 5(b), respectively, show the splitting due to the deuterium; the line resulting from the $F = 0$ level [shown in 5(c)] is not split. The experimental linewidth shown here is of the order of 10 kc/sec at a frequency of approximately 72 000 000 kc/sec. This is a better line Q than is achieved in the usual centimeter-wave maser. Doppler width at this frequency is about 200 kc/sec, which in the usual absorption spectrometer would completely obscure the deuterium coupling and would prevent evaluation of $(eQq)_D$ and C_D.

SPECTRAL FREQUENCIES AND MOLECULAR CONSTANTS

An improvement by two orders of magnitude in the rotational constants for HCN and DCN has been achieved. In the present work the frequencies are measured to an accuracy of about one part in 10^8.

The rotational transitions of $H^{12}C^{14}N$ are split by nuclear hyperfine structure due to the nitrogen nucleus. Although a slight splitting caused by

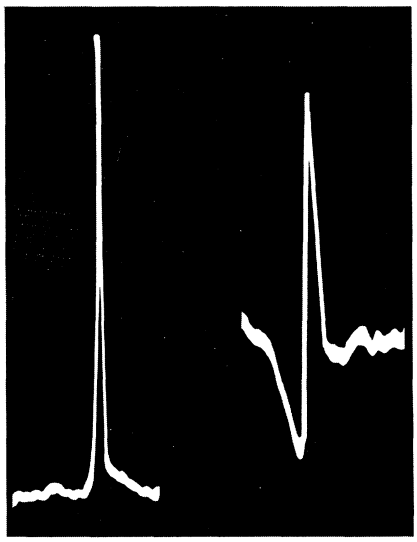

FIG. 4. Oscilloscope tracings of output of maser oscillator at 88.6 kMc/sec (left) and at 177.2 kMc/sec (right).

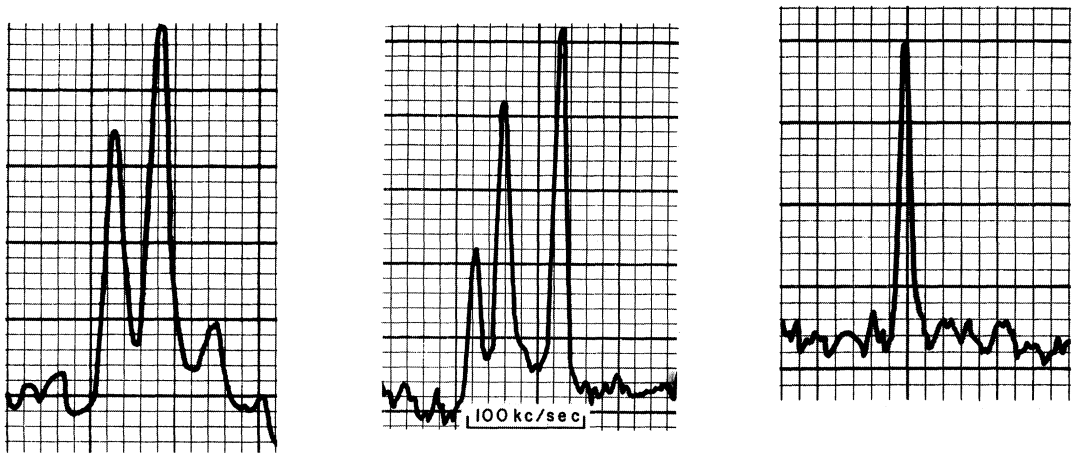

FIG. 5. $J=1\rightarrow 0$ spectrum of DCN showing the deuterium splitting of the nitrogen quadrupole lines. (a) $F=1$; (b) $F=2$; (c) $F=0$.

the magnetic coupling of hydrogen is expected, this was too small to be resolved. The nitrogen interaction gives rise to a triplet in the $J=1\rightarrow 0$ transition and to a sextet in the $J=2\rightarrow 1$ transition. Only five components of the sextet were measured. The weakest component, $F=1\rightarrow 2$, which is only $\frac{1}{2}\%$ of the total transition intensity, was not measured.

The energy formula, in frequency units, adequate to account for the observed frequencies is

$$E=E_R+E_Q+E_M\ , \tag{1}$$

where $$E_R=B_0J(J+1)-D_JJ^2(J+1)^2\ , \tag{2}$$

$$E_Q=-eQq\left(\frac{\frac{3}{4}C(C+1)-I(I+1)J(J+1)}{2I(2I-1)(2J-1)(2J+3)}\right), \tag{3}$$

$$E_M=\tfrac{1}{2}C_NC\ , \tag{4}$$

where $$C=F(F+1)-J(J+1)-I(I+1)\ , \tag{5}$$

$$F=J+\mathrm{I},\ J+I-1,\ \ldots,\ |J-I|\ , \tag{6}$$

and $$I=1,\ \text{for } {}^{14}\mathrm{N}. \tag{7}$$

In these expressions, $B_0=h/8\pi^2I_0$ is the usual rotation constant, D_J is the centrifugal stretching constant, $I=1$ is the spin, eQq is the nuclear quadrupole coupling constant, and C_N is the nuclear magnetic coupling constant of nitrogen. Because of the small values of the nuclear coupling constants and the large B_0 values, higher-order terms in E_Q and E_M do not produce observable effects. Higher-order effects in the centrifugal stretching are not detectable because of the small J values of the observed transitions. The values for the four spectral constants were obtained by a least-squares calculation of the difference between the measured line frequencies and the frequencies calculated from the spectral constants. This calculation was performed on an IBM 360/75 computer; the resulting fit of line frequencies is shown in Table I, and the spectral constants are given in Table II. The errors shown are statistical probable errors, based on a method due to Topping.[7]

The energy expression for DCN is appreciably more complicated than that for HCN, because of

TABLE I. Fitting of line frequencies of HCN (in kc/sec).

Transition		Observed	Calculated	$\Delta\nu$
$J=1\rightarrow 0$	$F=1\rightarrow 1$	88 630 415.7	88 630 414.7	1.0
	$F=2\rightarrow 1$	88 631 847.3	88 631 848.3	−0.9
	$F=0\rightarrow 1$	88 633 936.0	88 633 936.1	−0.1
$J=2\rightarrow 1$	$F=2\rightarrow 2$	177 259 676.7	177 259 677.4	−0.7
	$F=1\rightarrow 0$	177 259 923.3	177 259 923.3	0.0
	$F=2\rightarrow 1$	177 261 110.4	177 261 111.0	−0.6
	$F=3\rightarrow 2$	177 261 223.2	177 261 222.3	0.9
	$F=1\rightarrow 1$	177 263 445.0	177 263 444.7	0.3

TABLE II. Spectral constants of HCN and DCN from measurements with the molecular-beam maser (in kc/sec).

	$H^{12}C^{14}N$ Observed value	$D^{12}C^{14}N$ Observed value
B_0	44 315 975.7 ±0.4	36 207 462.7 ±0.2
D_J	87.24 ±0.06	57.83 ±0.04
$(eQq)_N$	−4 709.1 ±1.3	−4 703.0 ±1.2
C_N	10.4 ±0.3	8.4 ±0.3
$(eQq)_D$	•••	194.4 ±2.2
C_D	•••	−0.6 ±0.3

the additional nuclear coupling of deuterium. The analysis of the rotational hyperfine structure for a linear rotor having two nuclei with quadrupole coupling was originally worked out by Bardeen and Townes.[8] A more convenient expression for the secular matrix elements, which employs the tabulated 6J Wigner coefficients,[9] has been outlined by Thaddeus, Krisher, and Loubser.[10]

When magnetic as well as nuclear quadrupole interactions are included, the nuclear-interaction Hamiltonian for $D^{12}C^{14}N$ can be expressed as

$$\mathcal{H}_{\text{nucl}} = \mathcal{H}_Q(\text{N}) + \mathcal{H}_M(\text{N}) + \mathcal{H}_Q(\text{D}) + \mathcal{H}_M(\text{D}) \quad , \quad (8)$$

which has the specific value

$$\mathcal{H}_{\text{nucl}} = \frac{(eQq_J)_N}{2J(2J-1)I_N(2I_N-1)} \times [3(\vec{I}_N\cdot\vec{J})^2 + \tfrac{3}{2}(\vec{I}_N\cdot J) - \vec{I}_N^{\,2}\vec{J}^{\,2}] + C_N\vec{I}_N\cdot\vec{J} + \frac{(eQq_J)_D}{2J(2J-1)I_D(2I_D-1)} \times [3(\vec{I}_D\cdot\vec{J})^2 + \tfrac{3}{2}(\vec{I}_D\cdot\vec{J}) - \vec{I}_D^{\,2}\vec{J}^{\,2}] + C_D\vec{I}_D\cdot\vec{J} \quad , \quad (9)$$

where $$(eQq_J) = -(eQq)[J/(2J+3)], \quad (10)$$

and where q is the molecular-field gradient at the particular nucleus (nitrogen or deuterium) referred to the molecular axis. The usual quadrupole constants of nitrogen and deuterium are $(eQq)_N$ and $(eQq)_D$. The $\vec{I}\cdot\vec{J}$ terms represent the magnetic couplings, where C_N and C_D are the magnetic coupling constants for nitrogen and deuterium, respectively.

The solution of the two-quadrupole problem is facilitated by the choice of the proper coupling scheme. In this case, the appropriate coupling is

$$\vec{J} + \vec{I}_N = \vec{F}_N \quad , \quad (11)$$

$$\vec{F}_N + \vec{I}_D = \vec{F} \quad . \quad (12)$$

Since the nitrogen coupling is considerably larger than the deuterium coupling, this results in relatively small off-diagonal matrix elements. A single secular determinate was formed for the hyperfine levels of the $J=0$, 1, and 2 rotational states by use of the transformation formulas given by Thaddeus *et al.*[10] This results in a 19×19 matrix with undetermined coefficients. This was solved by the following procedure. Since the off-diagonal elements are small, a first-order least-squares fit is a good approximation to the final solution. The resulting first-order constants were then used for calculation of the matrix elements for the entire matrix. This matrix was then diagonalized, and the resulting calculated line frequencies compared with those obtained in the first-order fit. The differences in these values were then used for adjustment of the measured line frequencies before their reinsertion in the least-squares fit. The entire process was then iterated. At the end of each iteration, the original measured line frequencies were compared with the results of the diagonalization of the secular matrix. Convergence was obtained in about three iterations.

The resulting fit of line frequencies from this calculation is shown in Table III, and the spectral constants are shown in Table II.

Since the relation[11]

$$(C_N)_{DCN} = [(B_0)_{DCN}/(B_0)_{HCN}](C_N)_{HCN} \quad (13)$$

holds, an independent check of the accuracy of the spectral constants can be made. Substitution of the values found in this study for $(B_0)_{DCN}$, $(B_0)_{HCN}$, $(C_N)_{HCN}$ into Eq. (13) results in the value $(C_N)_{DCN} = 8.5$ kc/sec. In excellent agreement, and well within the stated probable errors, is the experimental value of 8.4 kc/sec. A similar procedure can be used for evaluation of the unobserved C_H:

$$C_H = [(B_0)_{HCN}/(B_0)_{DCN}](g_H/g_D)C_D \quad , \quad (14)$$

where g_H and g_D are the gyromagnetic ratios of the hydrogen and deuterium, respectively. Use of Eq. (14) and the results obtained for the DCN molecule reveals that $C_H = -4.8$ kc/sec. This small value explains the lack of observed hydrogen splitting in the HCN spectra.

The $J=0\rightarrow1$ transition of hydrogen cyanide was the first spectral transition to be observed with microwave methods at wavelengths below 4 mm. In the preliminary observations,[12] the frequency was measured with a cavity wavemeter only, but shortly thereafter, in 1949, the hyperfine multiplet of the $J=0\rightarrow1$ transition was measured[13] for both HCN and DCN with a precision frequency standard monitored by station WWV. A 30-Mc/sec error, due to an incorrect choice of frequency markers, was corrected in an erratum.[13] Because only the $J=0\rightarrow1$ transition was observed, the centrifugal stretching constant D_J could not be found. The infrared value of $D_J = 0.099$ Mc/sec was used in calculation of B_0. Nevertheless, the B_0 values thus determined in these early experi-

TABLE III. Fitting line frequencies of DCN (in kc/sec).

	Transition		Observed	Calculated	$\Delta\nu$
$J=1\rightarrow 0$	$F_N=1\rightarrow 1$	$F_D=1\rightarrow 0,1,2$	72 413 484.3	72 413 483.7	0.6
	$F_N=1\rightarrow 1$	$F_D=2\rightarrow 1,2$	72 413 514.3	72 413 514.1	0.2
	$F_N=1\rightarrow 1$	$F_D=0\rightarrow 0,1$	72 413 558.4	72 413 559.2	−0.8
	$F_N=2\rightarrow 1$	$F_D=1\rightarrow 0,1,2$	72 414 905.4	72 414 905.8	−0.4
	$F_N=2\rightarrow 1$	$F_D=3\rightarrow 2$	72 414 927.0	72 414 927.3	−0.3
	$F_N=2\rightarrow 1$	$F_D=2\rightarrow 1,2$	72 414 973.2	72 414 972.4	0.8
	$F_N=0\rightarrow 1$	$F_D=1\rightarrow 0,1,2$	72 417 029.7	72 417 029.7	0
$J=2\rightarrow 1$	$F_N=1\rightarrow 0$	$F_D=1\rightarrow 1$	144 826 841.4	144 826 841.2	0.2
	$F_N=1\rightarrow 0$	$F_D=2\rightarrow 1$	144 826 809.7	144 826 809.9	−0.2

ments result in line frequencies which are well within the error limits of ± 300 kc/sec for HCN and ± 200 kc/sec for DCN, as stated in the early work. Even so, the accuracy of the present value for B_0 for both $H^{12}C^{14}N$ and $D^{12}C^{14}N$ is more than two orders of magnitude greater than that of the earlier measurements. We believe that the present values for B_0 in HCN and DCN are the most accurate rotational constants determined for any molecule.

When instruments for higher millimeter and submillimeter frequencies became available, microwave measurements of the stretching constant D_J were made.[14] Although the previous value of 90.4 kc/sec for D_J in HCN is definitely too high, that of 57.4 kc/sec for D_J in DCN agrees very well with the present one. The earlier value of − 4.714 Mc/sec for $(eQq)_N$ that was obtained by Bhattacharya and Gordy[15] for HCN is in excellent agreement with the present maser value.

COMPARISON OF OBSERVED AND THEORETICAL VALUES OF $(eQq)_D$

Beginning with the work of Bassompierre,[16] several predictions of the field gradient at the hydrogen nucleus in HCN have been made with molecular orbital theory[17–19] by use of different basis functions. Previously, no reliable experimental test of these predictions could be made for the following reasons: Despite the fact that the nitrogen quadrupole coupling in HCN was known with good accuracy,[15] the field gradient q could not be derived with comparable accuracy from the measured $(eQq)_N$ because the value of quadrupole moment Q of nitrogen was relatively uncertain. For deuterium the reverse was true, i.e., the quadrupole moment of deuterium was accurately known, but the $(eQq)_D$ in DCN had not been measured with significant accuracy – only to ± 40%.[20] The present measurement of $(eQq)_D$ with the known Q provides a critical test of the molecular orbital calculations and assumed basis functions in DCN (or HCN).

Since it seems probable that the theory which predicts correctly the field gradient at the deuterium nucleus would also provide the best values for the field gradient at the N nucleus, this test also indirectly provides a more reliable value for the nitrogen quadrupole moment. The theory of Bonaccorsi, Scrocco, and Tomasi[19] predicts a value of 208 kc/sec for $(eQq)_D$, in good agreement with the experimental maser value. (See Table IV). Their theory with the observed value

TABLE IV. Comparisons of theoretical and observed deuterium quadrupole coupling of DCN (eQq in kc/sec).

Theoretical			
Kern and Karplus[a]	Mc Lean and Yoshimine[b]	O'Konski and Ha[c]	Bonaccorski, Scrocco, and Tomasi[d]
+310	+208.2	301.7, 239.8	208
Experimental			
White[e]			De Lucia and Gordy
±290 ± 120			194.4 ± 3

[a] C. W. Kern and M. Karplus, J. Chem. Phys. 42, 1062 (1965).

[b] Quoted by O'Konski and Ha, Ref. c.

[c] C. T. O'Konski and T.-K. Ha, J. Chem. Phys. 49, 5354 (1968).

[d] R. Bonaccorsi, E. Scrocco, and J. Tomasi, J. Chem. Phys. 50, 2940 (1969).

[e] L. White, J. Chem. Phys. 23, 253 (1953).

for $(eQq)_N$ leads to $Q(^{14}N) = 1.66 \times 10^{-26}$ cm^2. The recent evaluation by O'Konski and Ha[18] yields a value for $Q(^{14}N)$ of 1.56×10^{-26} cm^2, but their predictions of values for $(eQq)_D$ from different sets of basis functions (see Table IV), do not agree well with the measured value of $(eQq)_D$. These authors quote unpublished calculations by McLean and Yoshimine of $(eQq)_D = 208.2$ kc/sec and a resulting $Q(^{14}N) = 1.64 \times 10^{-26}$ cm^2, which agree with the predictions of Bonaccorsi *et al.*[19] A value of $Q(^{14}N) = 1.6 \times 10^{-26}$ cm^2 has been derived from the combined quadrupole and magnetic coupling in NO by Lin.[21] None of these derivations has included the Sternheimer correction.[22]

STANDARDS OF FREQUENCY AND WAVELENGTH FOR THE INFRARED REGION

Attempts have been made to obtain the speed of light by comparison of the B_0 value of HCN, measured in wavelength units by infrared techniques, with the microwave value of B_0, measured in frequency units.[23] As a result of the experiments reported here, the microwave value of B_0 is now about two orders of magnitude more accurate than the infrared-wavelength measurement, and is considerably more accurate than the value for the speed of light. A significant improvement in the infrared-wavelength measurement is needed to provide a better value of the speed of light. However, it seems unlikely that such an improvement will be made in the near future. Thus the most promising use of the present microwave value is its combination with the known speed of light to determine wavelength, or distance, more accurately.

One of the most important requirements for the useful development of the far-infrared region of the spectrum is the existence of accurate standards of frequency and wavelength. At present, the accepted standards are transition frequencies of CO, N_2O, and HCN.[24] These are derived from rotational spectral constants which are, in turn, derived from rotational-vibrational spectra in the near infrared. The spectral constants resulting from this beam-maser experiment are, however, considerably more precise than the infrared values; they can serve as improved standards of frequency, and when coupled with c, as wavelength standards for the far-infrared region.

---

†Work supported by the U.S. Air Force Office of Scientific Research, under Grant No. AF-AFOSR-66-0493A.

[1]J. P. Gordon, H. J. Zeiger, and C. H. Townes, Phys. Rev. 95, 282 (1954); 99, 1264 (1955).

[2]D. Marcuse, Proc. Inst. Radio Engrs. 49, 1706 (1961).

[3]A. F. Krupnov and V. A. Skvortsov, Zh. Eksperim. i Teor. Fiz. 47, 1605 (1964) [English transl.: Soviet Phys. – JETP 20, (1965)].

[4]F. De Lucia and W. Gordy (unpublished).

[5]L. O. Hocker, A. Javan, D. Ramachandra Rao, L. Frankel, and T. Sullivan, Appl. Phys. Letters 10, 5 (1967).

[6]V. Hughes and L. Grabner, Phys. Rev. 79, 829 (1950).

[7]J. Topping, Errors of Observation and Their Treatment (The Institute of Physics, London, 1956).

[8]J. Bardeen and C. H. Townes, Phys. Rev. 73, 97 (1948).

[9]M. Rotenberg, R. Bivens, N. Metropolis, and J. K. Wooten, The 3*j* and 6*j* Symbols (Technology Press, Cambridge, Mass., 1959).

[10]P. Thaddeus, L. C. Krisher, and J. H. N. Loubser, J. Chem. Phys. 40, 257 (1964).

[11]C. H. Townes and A. L. Schawlow, Microwave Spectroscopy (McGraw-Hill Book Co., New York, 1955).

[12]A. G. Smith, W. Gordy, J. W. Simmons, and W. V. Smith, Phys. Rev. 75, 260 (1949).

[13]J. W. Simmons, W. E. Anderson, and W. Gordy, Phys. Rev. 77, 77 (1950); 86, 1055(E) (1952).

[14]C. A. Burrus and W. Gordy, Phys. Rev. 101, 599 (1956).

[15]B. N. Bhattacharya and W. Gordy, Phys. Rev. 119, 144 (1960).

[16]A. Bassompierre, Discussions Faraday Soc. 19, 260 (1955).

[17]C. W. Kern and M. Karplus, J. Chem. Phys. 42, 1062 (1965).

[18]C. T. O'Konski and T.-K. Ha, J. Chem. Phys. 49, 5354 (1968).

[19]R. Bonaccorsi, E. Scrocco, and J. Tomasi, J. Chem. Phys. 50, 2940 (1969).

[20]R. L. White, J. Chem. Phys. 23, 253 (1955).

[21]C. C. Lin, Phys. Rev. 119, 1027 (1960).

[22]R. M. Sternheimer, Phys. Rev. 84, 244 (1951).

[23]D. H. Rank, J. Mol. Spectry. 17, 50 (1965).

[24]K. N. Rao, C. J. Humphreys, and D. H. Rank, Wavelength Standards in the Infrared (Academic Press Inc., New York, 1966).

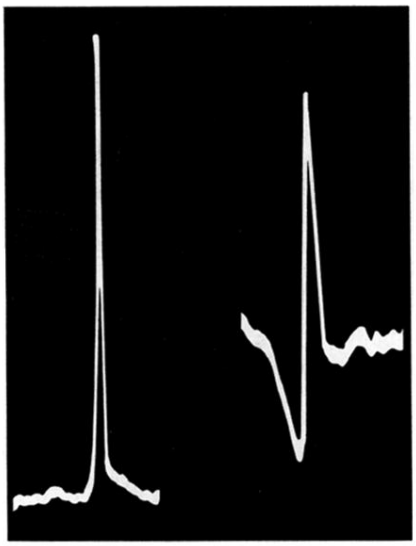

FIG. 4. Oscilloscope tracings of output of maser oscillator at 88.6 kMc/sec (left) and at 177.2 kMc/sec (right).